ACS APPLIED MATERIALS & INTERFACES

Research Article

www.acsami.org

Fabrication and Characterization of Stable Hydrophilic Microfluidic Devices Prepared via the in Situ Tertiary-Amine Catalyzed Michael Addition of Multifunctional Thiols to Multifunctional Acrylates

Christopher O. Bounds,[†] Jagannath Upadhyay,[‡] Nicholas Totaro,[†] Suman Thakuri,[‡] Leah Garber,[†] Michael Vincent,[†] Zhaoyang Huang,[§] Mateusz Hupert,[⊥] and John A. Pojman*[,†]

[†]Department of Chemistry, Louisiana State University, Baton Rouge, Louisiana 70303, United States

[‡]Department of Mechanical Engineering, Louisiana State University, Baton Rouge, Louisiana 70303, United States

[§]Department of Chemistry, Jacksonville University, Jacksonville, Florida 32211, United States

[⊥]Department of Chemistry, The University of North Carolina at Chapel Hill, Chapel Hill, North Carolina 27599, United States

Supporting Information

ABSTRACT: In situ tertiary amine-catalyzed thiol−acrylate chemistry was employed to produce hydrophilic microfluidic devices via a soft lithography process. The process involved the Michael addition of a secondary amine to a multifunctional acrylate producing a nonvolatile in situ tertiary amine catalyst/comonomer molecule. The Michael addition of a multifunctional thiol to a multifunctional acrylate was facilitated by the catalytic activity of the in situ catalyst/comonomer. These cost-efficient thiol−acrylate devices were prepared at room temperature, rapidly, and with little equipment. The thiol−acrylate thermoset materials were more natively hydrophilic than the normally employed poly(dimethylsiloxane) (PDMS) thermoset material, and the surface energies were stable compared to PDMS. Because the final chip was self-adhered via a simple chemical process utilizing the same chemistry, and it was naturally hydrophilic, there was no need for expensive instrumentation or complicated methods to "activate" the surface. There was also no need for postprocessing removal of the catalyst as it was incorporated into the polymer network. These bottom-up devices were fabricated to completion proving their validity as microfluidic devices, and the materials were manipulated and characterized via various analyses illustrating the potential diversity and tunability of the devices.

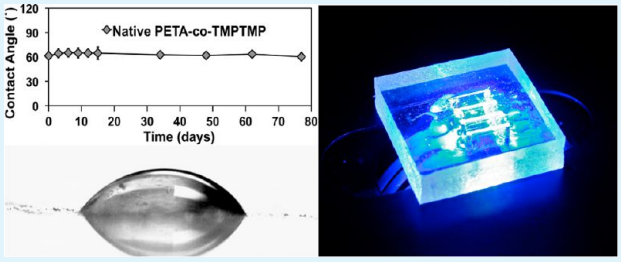

KEYWORDS: *microfluidics, soft-lithography, thiol-ene, hydrophilic, in situ catalyst*

INTRODUCTION

Thiol-ene Chemistry. The untapped potential of the simple and robust thiol-ene chemistry in various applications has only recently been realized. The majority of thiol-ene research has been directed toward photopolymerizable systems, and these reactions have been extensively studied.[1−10] The advantages associated with thiol-ene chemistry are legion. Many of the desirable properties of acrylic polymerizations as well as some unique properties are exhibited by thiol-ene polymerizations. Alternatively to photopolymerization mechanisms, a thiol-ene system can also undergo an ionic Michael addition polymerization mechanism utilizing a base catalyst; however, this type of reaction is limited to electron-deficient unsaturated enes, such as acrylates.[1,3,11,12] Although thiols are nucleophilic (generally more nucleophilic than amines), bases are used to deprotonate them because of their relatively high acidity. The thiolate anion is the active species formed by the thiol deprotonation that subsequently adds to an activated olefin such as an acrylate.[13] The rate of the thiol Michael addition increases with pH due to an increase in the thiolate anion concentration.[14] The rate is also dependent on the pK_a of the thiol with a more acidic thiol being more favorable. These acid−base reactions are thermodynamically controlled reactions that can occur spontaneously and can proceed to high conversion with an appropriate choice of thiol and catalyst.[15] Hu et al. used the predictable rise in pH facilitated by the formaldehyde-sulfite clock reaction to trigger the time-lapse Michael addition of a trithiol to a triacrylate.[16]

Thiol−acrylate systems can be catalyzed using tertiary amines, which function as base catalysts (Scheme 1). The tertiary amine deprotonates the thiol, forming thiolate anions that can add across acrylate double bonds to form the thiol-ene bond. However, these tertiary amine catalysts are relatively inefficient in the formation of such thiolate anions.[1,17]

Much more effective and efficient catalysts for the reaction between thiols and electron-deficient enes include primary

Received: November 1, 2012
Accepted: February 13, 2013
Published: February 13, 2013

Scheme 1. Tertiary Amine Catalyzed Thiol−acrylate Reaction Scheme

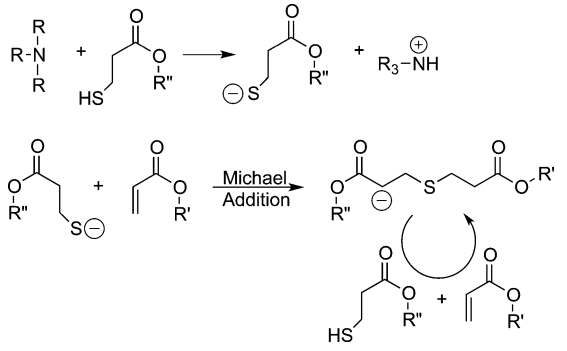

amines,[1,17] secondary amines,[17−23] or nucleophilic alkyl phosphine catalysts.[20,22] Bounds et al. utilized the rapid primary amine-initiated thiol-ene polymerization in the preparation of core-containing microparticles in less than 1 h at room temperature and ambient pressure.[24] Lee et al. used a secondary amine to catalyze the Michael addition of thiols to acrylates to produce novel vinyl ester monomers for photopolymerization kinetic studies.[18] Chan et al. reported producing a 1:1 reaction of thiol and acrylate to >95% conversion in less than 3 min in the presence of <2% primary or secondary amine.

Microfluidics. Microfluidics is a science associated with the processing and manipulation of small amounts of fluids via channels that range from tens to hundreds of micrometers.[25] Entire analytical protocols that have conventionally been executed in full-scale laboratories can be accomplished via miniaturized microfluidic systems.[26] Microfluidic devices, also referred to as micro total analysis systems (μTAS) or laboratories-on-a-chip (LOC), have recently found applications in areas such as DNA analysis,[27−29] protein assays,[30,31] air and water quality evaluations,[32] and clinical diagnostics.[33,34] Some of the obvious benefits of using microfluidic devices are their abilities to use microliter amounts of sample and reagents, their short reaction times, their minuscule analytical footprints, and their small, portable nature which all contribute to their high cost efficiency.[25,35] Other less obvious characteristics associated with μTAS include their high resolution and sensitivity, better reliability and functionality, a reduced risk of contamination, lower power consumption, laminar flow, and their capabilities of controlling concentrations of molecular species in both space and time.[25,26] Current technologies allow for a multitude of functions such as pretreatment, sample and reagent transport, reaction, separation, detection, and product collections to be implemented on a single μTAS.[26]

Casting of elastomeric materials[36−39] is perhaps the simplest way of replicating microstructures from a mold onto a polymer substrate. This technique, commonly referred to as soft lithography,[40−46] is most relevant for the work presented here. Soft lithography involves the pouring of a monomer solution (usually an elastomeric-forming monomer and a cross-linker) over a master mold, degassing of the solution, polymerizing (curing) at elevated temperatures, peeling the material from the mold, activating the surface, and adhering it to a flat surface, resulting in the final replicated microfluidic device.[39] This method can be used to prepare three-dimensional structures such as mixers,[47] valves,[48] and pumps.[49,50] This technique has many advantages including method simplicity, low cost, and replication accuracy.

Soft lithography of poly(dimethylsiloxane) (PDMS) is likely the dominant polymeric material-fabrication technique combination in the field of microfluidics.[51] This is due in part to the many useful properties of PDMS including its elastomeric nature, biocompatibility, gas permeability, optical transparency (down to 230 nm), moldability to submicrometer features, ability to be bonded to itself or glass, chemical inertness, and low cost of manufacturing.[26,52,53] Although PDMS has many advantages, it has a natively hydrophobic surface that expresses a water contact angle of ∼105°.[54] This hydrophobicity leads to many limitations especially in the field of biology where the majority of microfluidics is targeted. Cells avoid the hydrophobic surface of PDMS making it difficult to analyze cellular phenomena.[55] Proteins adsorb to the surface in a nonspecific manner making the native PDMS useless as a method of biomolecular separation assays.[56−58] From an obvious and practical standpoint, the hydrophobic surface of a PDMS also makes the introduction of aqueous solutions into small microchannels difficult.[51] PDMS, again due to its hydrophobicity, has a tendency to swell in some organic solvents causing difficulty in the analysis of various organic materials.[59] The surface of PDMS can be activated (oxidized) by oxygen plasma or ultraviolet treatments converting the hydrophobic silane-methyl groups to hydrophilic silane-hydroxyl groups. This hydrophilicity is only transient, however, as hydrophobic recovery is observed in as little as a few hours or days.[54,60] Improvements to the surface of PDMS have recently been realized via a multitude of surface modification techniques[61−68] resulting in stable hydrophilic surfaces. However, a natively hydrophilic material with similar properties to that of PDMS that could be used in a simple and inexpensive soft lithography process could be very useful as no modifications would be necessary to obtain the high energy surfaces achieved via modified PDMS materials.

The need and benefits of thiol-ene chemistry have been realized in the field of microfluidics but have been limited only to photopolymerizable systems. The unique aspects of the thiol-ene step-growth reaction make it superlative for photolithography and microfluidic device fabrication. More distinct photolithographic features can be obtained due to the delay in gel point associated with thiol-ene chemistry.[69] The network uniformity as well as the low shrinkage and shrinkage stress add some homogeneity and thus reproducibility to the final product.[2] The lack of oxygen inhibition facilitated by the thiol provides a less complex procedure where ambient conditions are required.[3] Photoinitiated thiol-ene systems have been used to fabricate microfluidic devices,[70−75] modify the surface of microdevices,[76] and control the material properties of microfluidic devices.[77,78] Good et al. used photoinitiated thiol-ene chemistry to prepare a flexible membrane removable lid for a gastight microfluidic device to separate an effervescent reaction from a sample.[74] Ashley et al. prepared microfluidic devices with a range of shapes and aspect ratios via a soft lithography process using photoinitiated thiol-ene and thiol−acrylate chemistries.[75] To prevent the normal instabilities of microfluidic devices in aliphatic and aromatic organic solvents, Cygan et al. fabricated organic solvent-resistant microfluidic devices using thiol-ene based resins via a rapid prototyping photolithography technique and quantified and explained their solvent resistance.[71] Natalie et al. prepared multilayer thiol-ene microfluidic devices by direct photolithographic patterning and transfer lamination avoiding the necessity for intermediate master molds and stamps.[72]

For the work described here, a method of using thiol-ene chemistry is described where all of the advantages associated with photoinduced thiol-ene chemistry were maintained, but the necessity for UV initiation was eliminated. A catalyst/commoner molecule was initially formed via the Michael addition of a secondary amine to a trifunctional acrylate. This resulting molecule was used as an in situ tertiary amine catalyst for the Michael addition of a multifunctional thiol to a multifunctional acrylate. By using this in situ catalyst pathway, further advantages were added to the already highly advantageous thiol-ene chemistry, especially in terms of biological systems and thus microfluidics. Amine catalyzed thiol−acrylate chemistry was used to prepare stable hydrophilic microfluidic devices in a simple fashion, in less time, and with out the need for expensive materials or instrumentation.

MATERIALS

All materials were used as received without further purification. Pentaerythritol triacrylate (PETA) was obtained from Sartomer and Sigma Aldrich. Trimethylolpropane tris(3-mercaptopropionate) (TMPTMP), diethylamine (DEA), and triethylamine (TEA) were obtained from Sigma-Aldrich. Polydimethylsiloxane was obtained from Dow Corning under the trade name Sylard 184. Structures for notable chemicals are illustrated in Scheme 2.

Scheme 2. Notable Chemical Structures for Microfluidic Device Fabrication

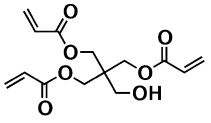

Pentaerythritol triacrylate

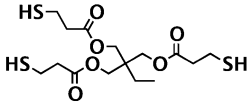

Trimethylolpropane tris(3-mercaptopropionate)

Diethylamine

Triethylamine

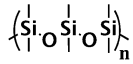

Polydimethylsiloxane

Fabrication Technique. Scheme 3 illustrates the generic soft lithography fabrication method used to prepare the thiol−acrylate microfluidic devices. Also shown here is a diagram for the soft lithography fabrication of a poly(dimethylsiloxane) (PDMS) microfluidic device for comparison purposes.[38,39] As with PDMS soft lithography, the thiol−acrylate (T-A) method is initiated by pouring the liquid thiol−acrylate/catalyst solution onto a poly(methyl methacrylate) (PMMA) positive mold. Unlike the PDMS method that must be heated to achieve rapid curing (1 h), the thiol−acrylate method gels in less than 1 h at room temperature. Next, both the PDMS and the T-A material can be peeled from the PMMA mold to yield a polymer negative. The surface of the PDMS material must then be modified via oxygen plasma for the adhering step and to produce a hydrophilic surface. The T-A material does not require any further surface modifications due to its native hydrophilicity and its ability to be adhered via the thiol−acrylate polymerization at the interface of the two materials. Detailed procedures can be found in the Supporting Information.

RESULTS AND DISCUSSION

Michael Addition to Produce in Situ Bound Catalyst. It was ideal for the applications of this polymeric material that it be easily produced under ambient conditions. Original samples were prepared using the simple tertiary amine, triethylamine. It was known[1] that tertiary amines such as triethylamine could act as a base catalyst for the thiol−acrylate reaction. However, thiol−acrylate film samples prepared using this highly volatile triethylamine had tacky surfaces when allowed to react open to the environment. It was hypothesized that the tacky nature was caused by the evaporation of the small molecular weight and highly volatile triethylamine resulting in low conversion at the surface of the film. To eliminate this problem, a less volatile tertiary amine that would not affect the hydrophilic nature of the product was sought. A secondary amine can act as a strong nucleophile in a Michael addition reaction with an electron-deficient acrylate.[13] Thus, a secondary amine, diethylamine, was attached to the high molecular weight acrylate (PETA) via a Michael addition resulting in a molecule that could function both as a nonvolatile catalyst and a comonomer containing available functionality to be cross-linked with the trithiol. Scheme 4 illustrates the simple Michael addition reaction scheme.

Scheme 4. Formation of in Situ Comonomer/Catalyst Molecule via the Michael Addition of a Secondary Amine to a Trifunctional Acrylate

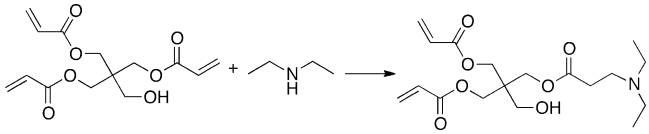

It was important to note that each addition of the secondary amine (DEA) to the trifunctional acrylate (PETA) caused a

Scheme 3. Basic Process for Soft Lithography Production of PETA-co-TMPTMP Boundless Microfluidic Device

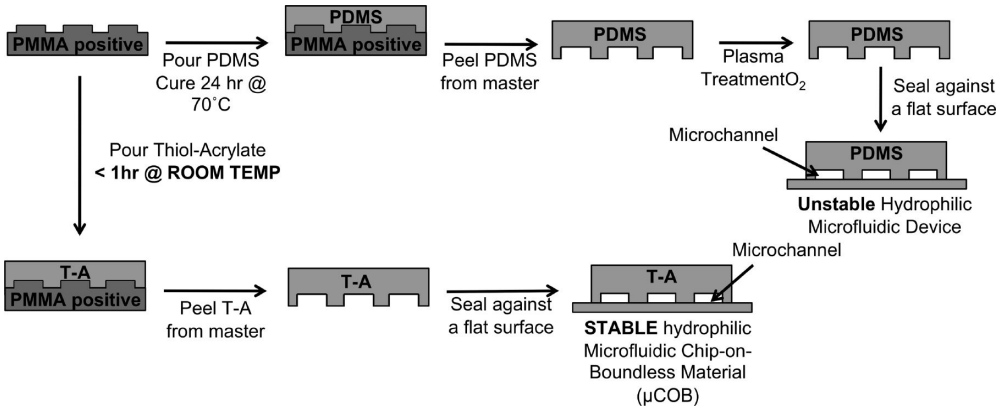

dx.doi.org/10.1021/am302544h | ACS Appl. Mater. Interfaces 2013, 5, 1643−1655

Scheme 5. Reaction Scheme Illustrating the Production of the Comonomer/Catalyst Molecule Followed by the Initiation and Two Propagation Steps of the Thiol−Acrylate Michael Addition

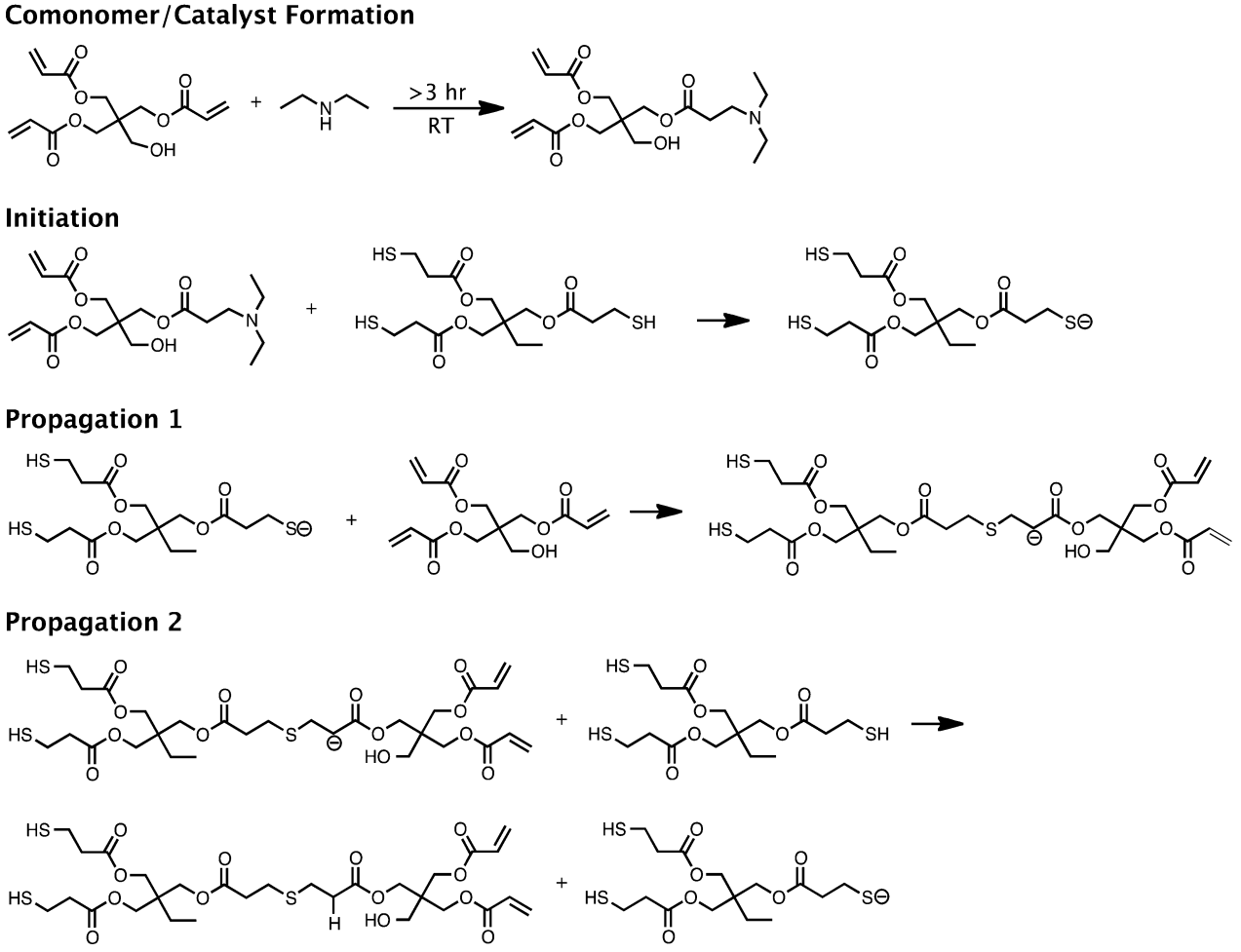

decrease in the average functionality of the comonomer thiol−acrylate system. With each addition, a trifunctional acrylate molecule became a difunctional acrylate molecule. Because this reaction proceeds via a step-growth mechanism, an average functionality greater than two was required to achieve a cross-linked network. It was therefore imperative that the DEA concentration not reach a value that would result in the decrease of the average monomer functionality to below two.

In order to confirm this reaction and determine the simple reaction kinetics, the reaction conversion was studied as a function of time. The decrease in the acrylate peak of PETA was monitored via NMR analysis. The results can be found in Supplemental Figure 1, Supporting Information. The peaks corresponding to the acrylate groups decreased by ∼20% upon the reaction of PETA and DEA for 3 h. This suggested quantitative conversion of the secondary amine to a tertiary amine catalyst/comonomer molecule via the Michael addition of diethylamine to the electron deficient acrylate. Virtually all of the secondary amine was converted to a tertiary amine in 3 h. Because of this result, the diethylamine and PETA were allowed to react for at least 3 h prior to the addition of the trithiol (TMPTMP) and the completion of the final product. Unless otherwise noted, the typical comonomer/catalyst solution contained 16.1 mol % DEA by functional group.

Addition of the Comonomer/Catalyst to the Multifunctional Thiol. Once the in situ catalyst was produced, it was added to the trithiol (TMPTMP) in a stoichiometric 1:1 molar ratio of thiol to acrylate functional groups. This molar ratio accounted for the amount of acrylate groups consumed during the initial Michael reaction with the secondary amine. Thus, the final amount of thiol added to the reaction mixture was not based on the initial amount of acrylate groups incorporated, and the amine concentrations are all given with respect only to the acrylate functional groups and not to the total mixture.

Scheme 5 illustrates the suspected reaction from the initial Michael reaction producing the high molecular weight, nonvolatile tertiary amine catalyst to the initiation and propagation of the thiol−acrylate polymerization. The tertiary amine catalyst functioned as a strong base to deprotonate the thiol, resulting in the initiation of the anionic step-growth polymerization mechanism. Two separate propagation steps then followed. The first propagation step involved the Michael Addition of the deprotonated thiyl anion to the electron-deficient ene group. Next, a hydrogen transfer occurred between another thiol and the newly formed carbon anion. This second propagation step resulted in a chain transfer and another deprotonated thiol that was activated for another Michael Addition. This dual propagation mechanism is the reason that this reaction is considered a step-growth polymerization; however, it is essentially a chain-growth mechanism

dx.doi.org/10.1021/am302544h | ACS Appl. Mater. Interfaces 2013, 5, 1643−1655

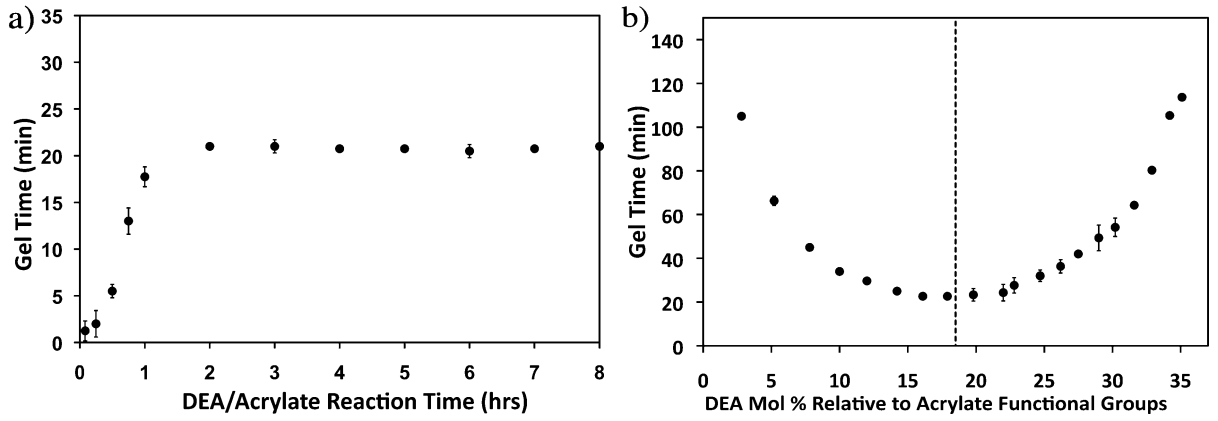

Figure 1. Thiol–acrylate gel time as a function of (a) DEA/PETA reaction time (system containing 16.1 mol % DEA) and (b) diethyl amine concentration. DEA concentrations are with respect to the acrylate functional groups only. The DEA/PETA solution was allowed to react for 24 h prior to the addition of the trithiol for panel b.

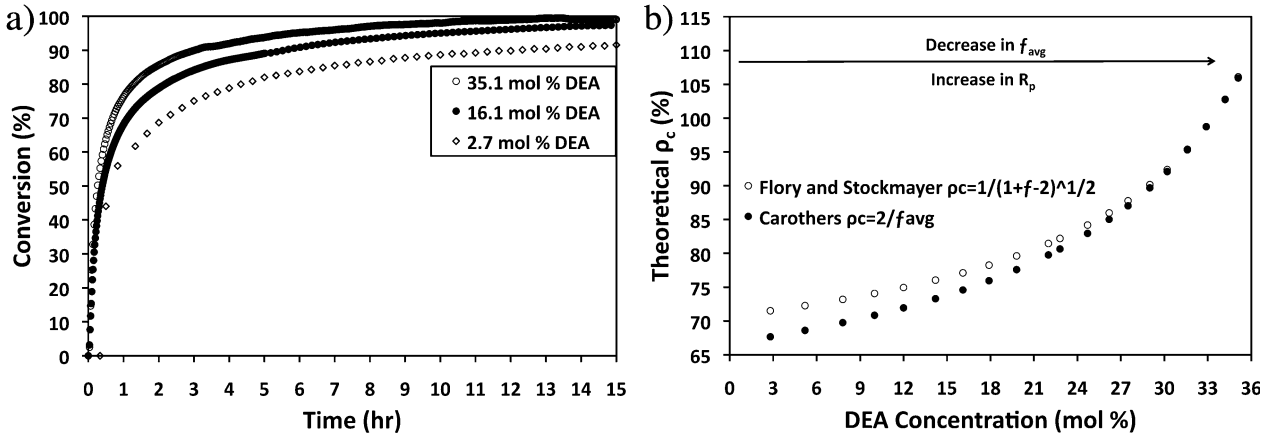

Figure 2. Conversion data as a function of amine concentration. Panel a illustrates the real-time conversion of acrylate functional groups monitored via FTIR as a function of amine catalyst concentration. Panel b illustrates the theoretical critical conversion value as a function of the fraction of acrylate groups previously reacted (DEA concentration) using both the Flory and Stockmayer estimation and the Carothers estimation.

with a continuously sequential chain transfer step (propagation 2).

Gel Times as a Function of DEA-PETA Reaction Time and DEA Concentration. The thiol–acrylate experimental gel times were determined as a function of DEA/PETA reaction time. This was necessary to determine the time required to reach high conversion of the nonvolatile tertiary amine prior to the addition of the trithiol. The experimental gel times were in agreement with the NMR data.

Figure 1a illustrates the experimental gel time for the thiol–acrylate material as a function of the elapsed reaction time associated with the initial amine-acrylate Michael addition. The experimental gel time was defined as the point at which an air bubble could no longer rise through the material. The gel time increased as a function of the amine-acrylate reaction time until a point after which the gel time stabilized. The increase in the gel time as a function of DEA/PETA reaction time was due to the differences in the catalytic abilities of tertiary and secondary amines.[19] Chan et al. have shown that a primary amine or a secondary amine can function as a nucleophilic- and more efficient catalyst for the thiol–acrylate reaction compared to a tertiary amine base catalyst.[1] The increase in the thiol–acrylate gel time as a function of time is indicative of a conversion of a secondary amine to a tertiary amine. As the secondary amine was converted to a tertiary amine, the catalyst mechanism shifted from a nucleophilic catalysis to a less efficient base catalysis. Once the gel time reached a steady state, all of the nucleophilic secondary amine had been converted to a tertiary amine base catalyst. According to the experimental gel times, the DEA/PETA reaction was complete in ~2 h as indicated by the constant gel times reached beyond 2 h. This was consistent with the NMR data in Supplemental Figure 1, Supporting Information, and with our hypothesis that the initial amine-acrylate Michael reaction did occur and reached completion in 2–3 h. Because of the experimental gel time data and the NMR data, each DEA/PETA reaction was allowed to proceed for at least 3 h under constant stirring prior to the addition of the trithiol.

The thiol–acrylate gel time could be manipulated by varying the concentration of DEA incorporated. Figure 1b illustrates the gel time as a function of initial amine concentration. The manipulated gel times ranged from ~2 h to <20 min within the amine concentration range examined in this study. The DEA/PETA stock solution was allowed to react for 24 h prior to the addition of the trithiol in each case illustrated in Figure 1b. The left half of Figure 1b conforms to the normally accepted catalyst concentration trend. As the concentration of catalyst was increased, the reaction rate increased causing a decrease in the gel time. However, beyond ~17 mol % DEA, the gel time began to increase, which would apparently indicate an

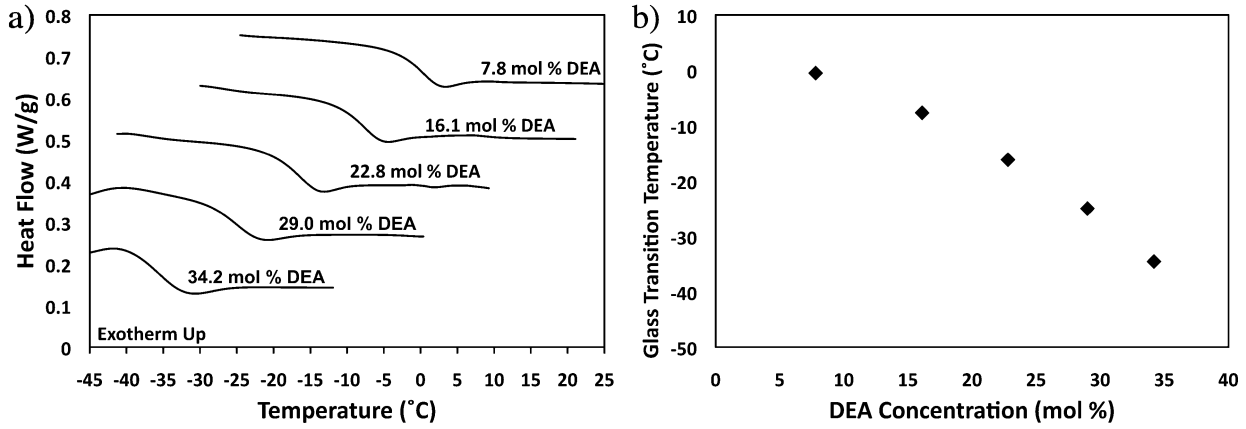

Figure 3. Differential scanning calorimetry data showing glass transition temperatures (T_g). Panel a illustrates the heat flow as a function of temperature at varying DEA concentrations. Panel b illustrates the glass transition temperature as a function of DEA concentration.

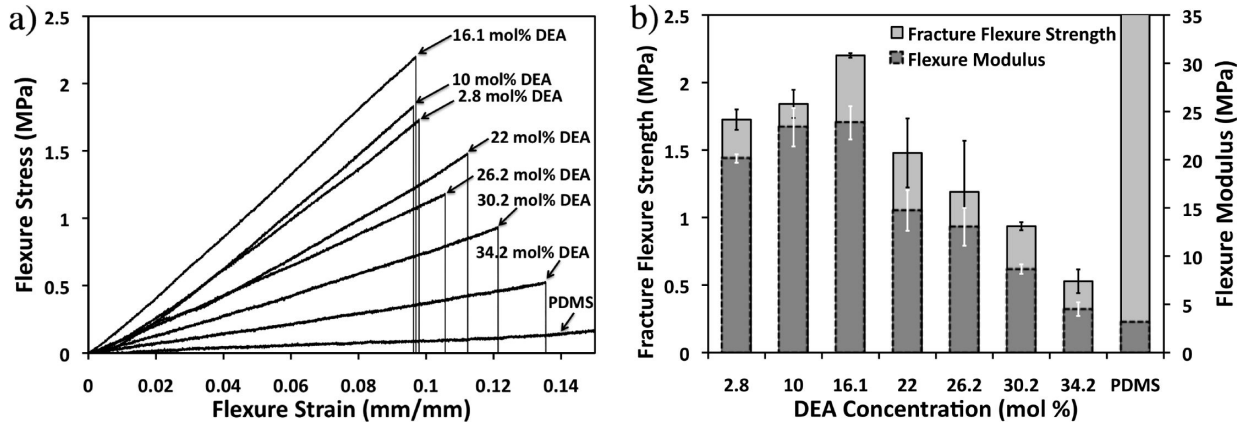

Figure 4. 3-point bending analysis results. (a) Stress strain curve as a function of DEA concentration; (b) fracture flexure strength and flexure modulus as a function of DEA concentration. All samples were tested after 24 h.

uncommon decrease in the rate of polymerization with an increase in catalyst concentration. It could be argued that this was simply due to a dilution effect, declaring that at some point the catalyst diluted the acrylate and thiol functional groups causing a decrease in the rate of polymerization. It could also be argued that the loss of acrylate functional groups associated with the first Michael addition caused a decrease in the rate of polymerization with an increase in the amine concentration. When the decrease in monomer concentration outweighed the increase in the rate constant caused by an increase in catalyst concentration, the overall rate of polymerization decreased. However, both of these arguments were falsified via FTIR analysis, and the conversion kinetics of this in situ thiol–acrylate polymerization reaction were determined.

Gel Time Analysis Via FTIR. To address the unusual gel time observation as a function of DEA concentration previously addressed (Figure 1b), the thiol–acrylate kinetics were studied as a function of amine catalyst concentration. Figure 2a illustrates these data.

The data in Figure 2a show that the rate of polymerization increased as a function of DEA concentration disproving the arguments discussed previously. Therefore, a different explanation was hypothesized where the average functionality of the monomer/catalyst molecule was the determining factor of the unusual gel times. The critical conversion required to reach gelation (ρ_c) can be estimated on the basis of two different theories, the Carothers theory[79] and the Flory and Stockmayer theory,[79] both equations shown below:

Carothers:

$$\rho_c = 2/f_{avg}$$

Flory and Stockmayer:

$$\rho_c = 1/(1 + f - 2)^{1/2}$$

These theories assume equal reactivity of all functional groups of the same type regardless of the size of the molecule and that there are no intramolecular reactions between functional groups on the same molecule.[79] Because of this assumption, the theoretical numbers may not exactly match the experimental data, but the overall trend should. As shown in Figure 2a, the rate (R_p) of loss of monomer increased with an increase in the concentration of amine; however, the gel time (Figure 1b) increased with an increase in the concentration of amine. In this case, the increase in the gel time with extremely high amine concentration was associated with a change in the critical percent conversion (ρ_c). As the concentration of the amine was increased, the functionality of the acrylate was decreased due to the initial Michael reaction, causing ρ_c to increase greatly thereby preventing gelation until later in the reaction. This was the cause of the decrease in the gel time as a function of the increase in catalyst concentration at high concentration and the parabola-type curve shown in Figure 1b.

This resulted in the illusion of a decrease in the rate of polymerization. The physical gel times of these particular thiol−acrylate reactions could be manipulated to a point, but a lower limit did exist due to the use of an in situ catalyst that inherently caused a decrease in the average functionality of the system.

Glass Transition Measurements. Differential scanning calorimetry was performed on these thiol−acrylate materials to determine their glass transition temperatures. Figure 3 illustrates the glass transition temperatures at different amine catalyst concentrations. Figure 3a shows the raw DSC data of heat flow as a function of temperature. The second-order transition temperatures are easily observed where the heat flow decreased at a given temperature without recovering back to the original baseline. Figure 3b illustrates the measured glass transition temperature as function of amine concentration. The DSC data provided the working temperatures associated with these thiol−acrylate materials via the determination of the glass transition temperatures (T_g). The useable-temperature of the material could be manipulated on the basis of the concentration of the in situ amine catalyst. All of the combinations observed in Figure 3 showed glass transition temperatures of less than 0 °C. The change in the glass transition temperature as a function of DEA concentration (Figure 3b) was attributed to the decrease in the cross-link density with an increase in the DEA concentration. From a microfluidic standpoint, the natively low and manipulatable T_g of these materials is advantageous as it allows for a wide analyte temperature range to be employed during analysis.

Flexure Strength. The flexure strengths of these thiol−acrylate materials were determined using a 3-point bending method. The mechanical properties of the material were manipulated as via alterations in the amine concentration as shown in Figure 4. Beyond 16.1 mol % DEA, the flexure strength of the material (Figure 4b) decreased and the flexibility (Figure 4b) increased with an increase in the DEA concentration. The increase in flexibility and the decrease in flexure strength originated from the decrease in the cross-link density facilitated by the increase in the concentration of the amine. Again, due to the first Michael addition, an increase in the amine concentration caused a decrease in the functionality of the trifunctional acrylate, resulting in a decrease in the overall functionality and thus the cross-link opportunities. The material with the highest flexure strength and modulus was that containing 16.1 mol % DEA. Since there was a slight decrease in the flexure strength and modulus of materials containing less than 16.1 mol % DEA, the reaction conversion also likely played a role in the strength of the material. All of the samples used in the analysis were allowed to react for 24 h prior to being tested. The material with the highest strength and modulus was also the material with the fastest gel time (gel time Figure 1b). This potentially implied that the polymerization kinetics played a role in the strength of the final material.

PDMS samples of the same dimensions were also analyzed using this 3-point bending technique. The data for these silicone samples are shown in Figure 4. The PDMS materials were found to have much higher flexure fracture strength. Because the 3-point bending technique employed was not successful in fracturing the samples, Figure 4a illustrates the continuation of the stress strain curve infinitely along the *x*-axis, and Figure 4b illustrates the continuation of the corresponding strength data bar beyond the scope of the measurement along the *y*-axis. The PDMS samples also boasted a very low flexure modulus only attainable via a PETA-co-TMPTMP sample with very low flexure strength. These data indicated that, in terms of material strength, PDMS was much stronger and much more flexible than the PETA-co-TMPTMP samples. This material weakness compared to PDMS may not be a significant disadvantage, as the field of microfluidics does not require extremely tough and rugged materials for biological assays.

To determine if there was a kinetic aspect in correlation with the mechanical strength of the material, the mechanical properties of a typical sample produced using 16.1 mol % DEA were analyzed as a function of elapsed time beyond the gel time. These data are shown in Figure 5. Both the strength and stiffness of the material increased as a function of elapsed time from 1 to 24 h. Beyond 24 h, the strength and flexibility of the material remained constant, indicating that the full strength of the material could be obtained after 24 h of reaction time. This was in full agreement with the kinetic data (Supplemental Figure 1a, Supporting Information), as the reaction was observed to reach >95% conversion after a 24 h time period.

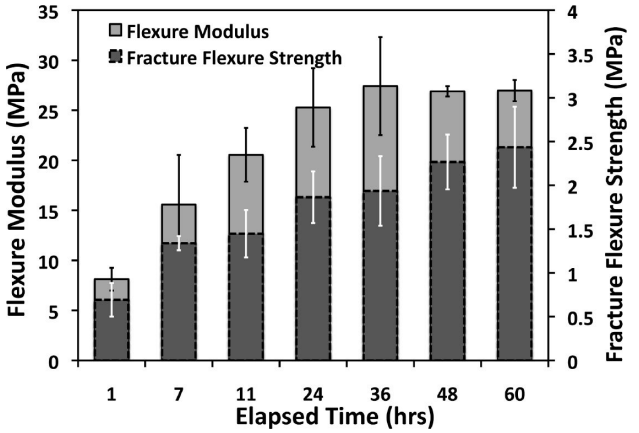

Figure 5. 3-point bending analysis results illustrating the flexure modulus and the flexure strength as a function of elapsed time after polymerization. The studied samples were composed of 16.1 mol % DEA relative to the acrylate functional groups.

Bonding via Partial Polymerization/Excess Monomer Technique. Two thiol−acrylate sections could be bonded using the same chemistry without the need for surface activation. The adhesion was facilitated via a partial polymerization method involving excess functional groups on opposing surfaces. Scheme 6 illustrates the microfluidic device annealing mechanism.

The adhesion between the two surfaces was attributed to the extremely high conversion associated with thiol−acrylate chemistry as well as the use of a step-growth mechanism where the gel time was rapid, but the full conversion was relatively slow. The excess acrylate on one surface and excess thiol on the other resulted in a net 1:1 molar ratio of thiol to acrylate functional groups between the two surfaces. This then allowed for the same Michael addition of thiol to acrylate, again catalyzed by the in situ tertiary amine previously incorporated into the network. The covalent thiol−carbon bond produced a strong adhesion between the surfaces resulting in sealed microfluidic channels down which water could confidently be pumped.

In order to determine the strength of the bond formed using this partial polymerization method, the orthogonal force

Scheme 6. Bonding of Thiol Acrylate Microfluidic Device via a Partial Polymerization and Excess Monomer Method

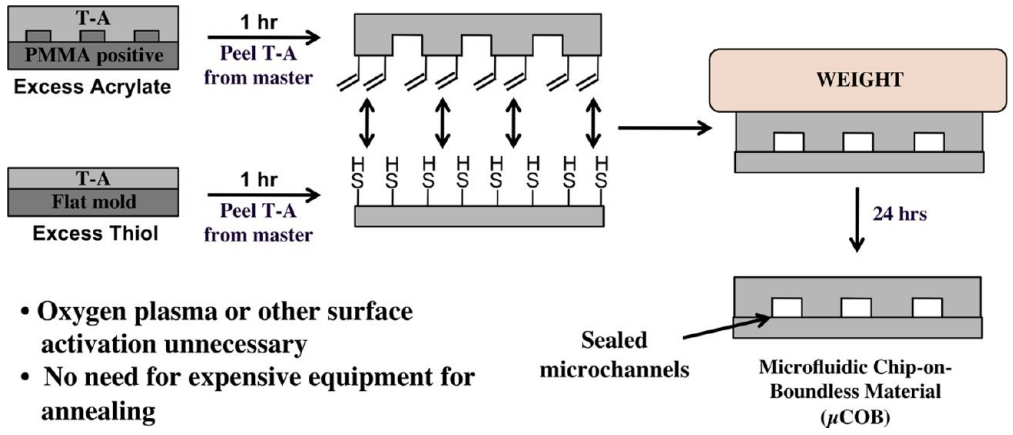

necessary to delaminate the bonded surfaces was determined. These data are shown in Figure 6.

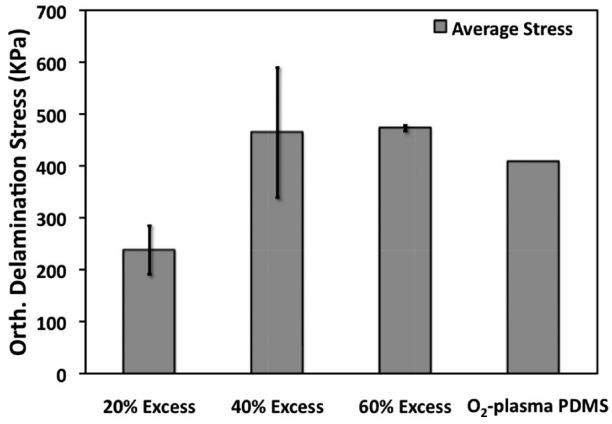

Figure 6. Adhesive bond strength as a function of excess monomer (thiol and acrylate) compared to the adhesive bond strength of oxygen plasma activated PDMS.

Flat samples were employed for ease of comparison. Figure 6 illustrates an increase in the average required delamination force as a function of increasing excess monomer concentration from 20% excess monomer to 40% excess monomer. There was little difference in the average strength of the annealing bond above 40% excess monomer. This was attributed to the different types of failures experienced by the polymer samples. Two annealed samples could be delaminated at the surface of the material via an adhesive failure where the strength of the bond was dependent on the strength of the adherence at the interface of the two materials. Samples could also fail in a cohesive manner where the adhesive surface bond was stronger than the material being adhered. The samples containing 20% excess monomer (Figure 7a) suffered adhesive failure, while both the samples containing 40% (Figure 7b) and 60% excess monomer (Figure 7c) experienced cohesive failure.

At excess monomer concentrations below 40%, the fewer number of covalent bonds between the two films limited the strength of the bonding. Beyond 40% excess monomer, the strength of the bond was limited only by the mechanical strength of the material, thus no change in the average stress was observed from 40% to 60% excess monomer. There was, however, an apparent increase in the reliability of the bond at 60% excess monomer, as the standard deviation was lower when 60% excess monomer was utilized (Figure 5). The error decreased when 60% excess monomer was used because there was a more uniform bond between the two flat surfaces due to the increase in the number of thiol−acrylate bonds produced. The reasoning behind the sporadically higher delamination stresses in some cases where 40% excess monomer was used was not well understood.

Again for comparison purposes, bonded PDMS samples were exploited via the same orthogonal delamination analysis. Both PDMS pieces were first exposed to an oxygen plasma generator for 30 s to activate the surface for annealing. The PDMS materials were then pressed together and placed in an oven for 24 h at 37 °C. The average bond strength of the thiol−acrylate materials containing 40% and 60% excess monomer were

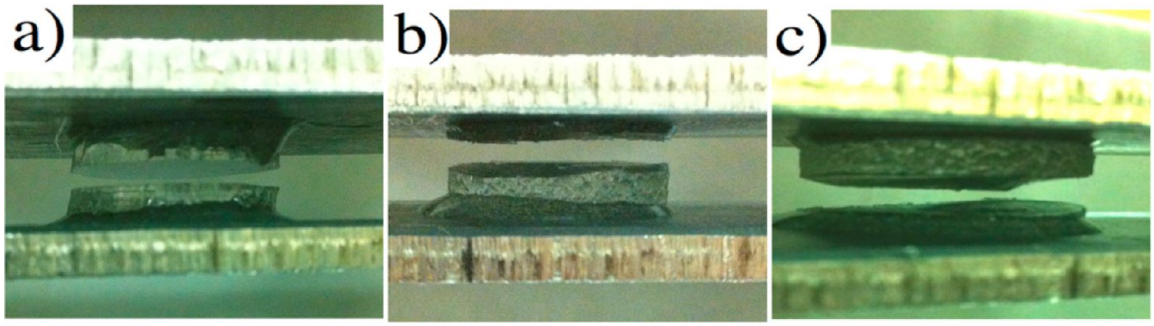

Figure 7. Images of experimental orthogonal delamination failure results, (a) 20% excess monomer, (b) 40% excess monomer, and (c) 60% excess monomer.

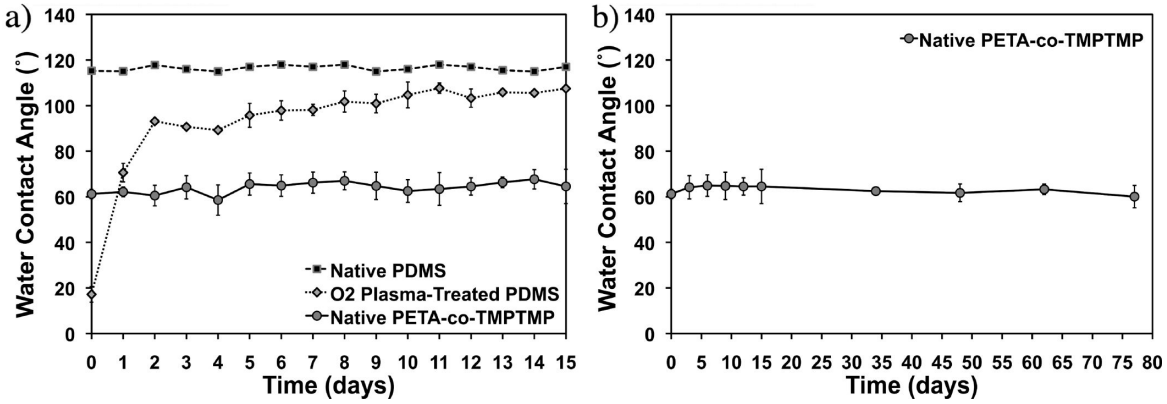

Figure 8. Water contact angle as a function of time for (a) 2 weeks illustrating native PETA-co-TMPTMP, native PDMS, and PDMS exposed to oxygen plasma for 30 s and (b) 2.5 months showing only native PETA-co-TMPTMP.

comparable to that of two PDMS materials bonded using the oxygen plasma treatment. Therefore, a thiol−acrylate microfluidic device could be prepared with the same bond integrity as that of a PDMS device without the need for expensive instrumentation such as an oxygen plasma generator.

The excess monomer concentration present due to the employed partial polymerization technique did not significantly alter the material properties of the resulting product. However, if the materials were slightly affected by this excess monomer, it has been illustrated that the material properties can easily be manipulated. Changes in the cross-link densities of these materials via amine concentration manipulation can produce materials with various material properties.

Native Contact Angles. One of the most useful properties of this copolymer material in terms of microfluidic applications is its stable hydrophilic surface. Hydrophilicity is a very useful and sometimes necessary property of microfluidic devices for a multitude of reasons.[51,55−58] One obvious advantage is the wettability of the surface. A hydrophilic surface allows for the passage of aqueous materials down small microchannels (or nanochannels) with little force as opposed to small hydrophobic channels.[51] Some polymer materials used in microfluidics can be modified to allow for lower contact angles, such as oxygen plasma treatment to PDMS,[60] which results in drastic decreases in the water contact angle. However, the surfaces of these oxygen plasma treated samples are not stable beyond a few days and eventually return to their hydrophobic state.[60] Therefore, a stable microfluidic device is a highly desirable novel feature, as this would facilitate a prolonged shelf life. The water contact angles of these native thiol−acrylate copolymers were observed to range from ∼60 to 65° regardless of the time elapsed after polymerization or the trithiol concentration. Supplemental Figure 4a,b, Supporting Information, visually illustrates a water droplet on a native PDMS surface and on a native PETA-co-TMPTMP surface, respectively. It was obvious from the optical microscopy images that the thiol−acrylate surface was much more hydrophilic (wettable) compared to the PDMS substrate.

The native PDMS surface had a hydrophobic water contact angle of ∼115° as opposed to the hydrophilic thiol−acrylate native contact angle of ∼60°. Figure 8 illustrates the water contact angles of native PDMS, oxygen plasma treated PDMS, and PETA-co-TMPTMP as a function of time. Native PDMS had a hydrophobic surface with a water contact angle of ∼115° that remained constant for 2 weeks (Figure 8a). A PDMS sample exposed to oxygen plasma for 30 s showed initial hydrophilicity, having a water contact angle of <20° immediately following the oxygen plasma treatment. This hydrophilicity was only transient, however, as the surface quickly recovered back to its hydrophobic state with a contact angle of ∼70° after 1 day, >90° after 2 days, >100° after 1 week, and >107° after 2 weeks (Figure 8a). The PETA-co-TMPTMP sample, on the other hand, exhibited a stable hydrophilic surface with an initial water contact angle of ∼60° that remained constant within 6° over the same 2 week time period (Figure 8a).

The surface of the native PETA-co-TMPTMP material was monitored for ∼2.5 months to determine the longevity of its stable surface (Figure 8b). Throughout the extended study, the water contact angle remained constant within 6° for 2.5 months. The initial average water contact angle on day 1 was 61°, and the final average water contact angle on day 77 was 60°. Therefore, it was proven that this native thiol−acrylate microfluidic material could have a shelf life of at least 2.5 months, and there was little reason to expect any variations in the surface for even longer periods of time.

The native water contact angles were also determined as a function of monomer concentration. This was a crucial factor in correlation with the bonding of the material. Because the materials were bonded using an excess monomer method, it was important to know the effect of the monomer concentration on the surface properties of the material. This data can be found in the Supporting Information. The water contact angle was observed to be independent of the concentration of trithiol incorporated. This proved that the method used to bond the two surfaces did not negatively affect the surface properties of the material with respect to hydrophilicity.

Water Mass Uptake of Native PETA-co-TMPTMP Materials. Due to the hydrophilic nature of these native thiol−acrylate materials, some water mass uptake was expected. It was important to determine the water mass uptake as this could alter the size of the microchannels over time. This "swelling" could also be very beneficial as smaller dimensions could be obtained via shrinkage of the microchannels to produce even nanodimensions via a postprocessing swelling technique. The native thiol−acrylate samples were completely submerged in distilled water, removed and weighed periodically, and again submerged repeatedly for a lengthy 4-month study. The water mass uptakes at various time intervals and different amine catalyst concentrations were determined. This data can be found in the Supporting Information. For samples

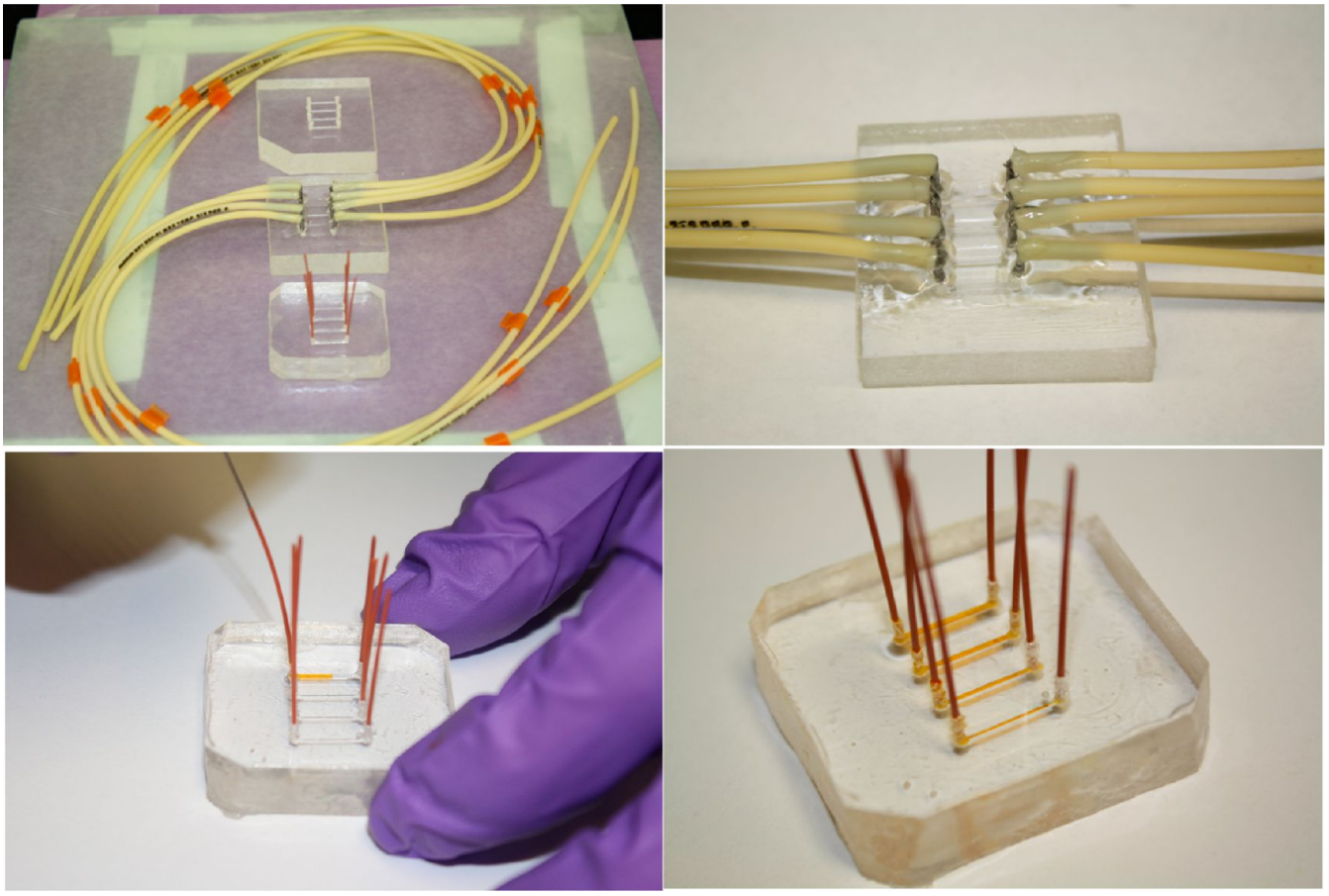

Figure 9. Images of final, annealed PETA-co-TMPTMP microfluidic devices attached to inlet capillaries (top left and top right) and an aqueous methyl orange solution being pumped through a final, annealed PETA-co-TMPTMP microfluidic device (bottom left and bottom right).

containing 1.35 mol % DEA, after 30 min of water exposure time, an average mass increase was documented at 0.19%. From there, the percent mass uptake increased over time to 0.80%, 1.0%, 1.5%, and 3.1% after 1 day, 2 days, 12 days, and 4 months, respectively, when 1.35 mol % DEA was used. Because normal microfluidic applications involve only short transient interactions with aqueous solutions, only the water mass uptake at relatively low water exposure times were relevant. It was concluded that the water mass increases associated with these native thiol−acrylate materials were negligible as the material absorbs ≤1% of its mass after 2 days fully submerged in water.

There was a correlation between the water mass uptake and the concentration of the amine catalyst at long submersion times. No change in the mass uptake was observed, within the standard deviation, of samples containing different concentrations of amine when submerged in water for 2 days or less. However, at submersion times ≥12 days, there was an increase in the water mass uptake with an increase in the amine concentration. The average mass uptake for samples containing 2.65 mol % DEA was 2.1% after 12 days and 6.0% after 4 months. This was expected as an increase in the concentration of the amine caused a decrease in the average functionality of the system and thus a decrease in the cross-link density of the material. Because the hydrophilic material was less cross-linked at higher amine concentrations, more water could interpenetrate the network causing an increase in the mass uptake over time. Even at the higher concentration of amine, there was still very little mass increase at submersion times of ≤2 days. After 2 days of full submersion time, the material containing 2.65 mol % DEA experienced a mass increase of 1.2%. Regardless of the amine concentration, there was little, if any, substantial water mass increase over the time period of interest for microfluidic applications using this native thiol−acrylate material.

Solvent Mass Uptake of Native PETA-co-TMPTMP Materials vs Native PDMS. It was desirable to know how the thiol−acrylate materials would react in solvents that typically cause severe swelling of PDMS. The native thiol−acrylate samples as well as PDMS pieces of the same dimensions were completely submerged in cyclohexane, hexane, or triethylamine, removed and weighed periodically, and again submerged repeatedly for a 1-week study. The solvent mass uptakes at various time intervals can be found in Supplemental Figure 7, Supporting Information. It was clearly noted that the thiol−acrylate materials experienced far less solvent uptake in each solvent studied. For example, after 30 min of exposure to cyclohexane, hexane, and triethylamine, the PDMS had experienced average mass increases of 65%, 62%, and 50%, respectively. The PETA-co-TMPTA samples, on the other hand, experienced only 0.2%, 0.05%, and 0.02% when exposed to cyclohexane, hexane, and triethylamine for 30 min, respectively. After 1 week of triethylamine exposure time, PDMS illustrated a 550% increase in mass while PETA-co-TMPTMP experienced only 1.4% mass increase under the same conditions. It was concluded that the thiol−acrylate materials were much more resilient in terms of solvent resistance. Regardless of the solvent utilized, the PETA-co-TMPTMP greatly outperformed the PDMS in terms of solvent

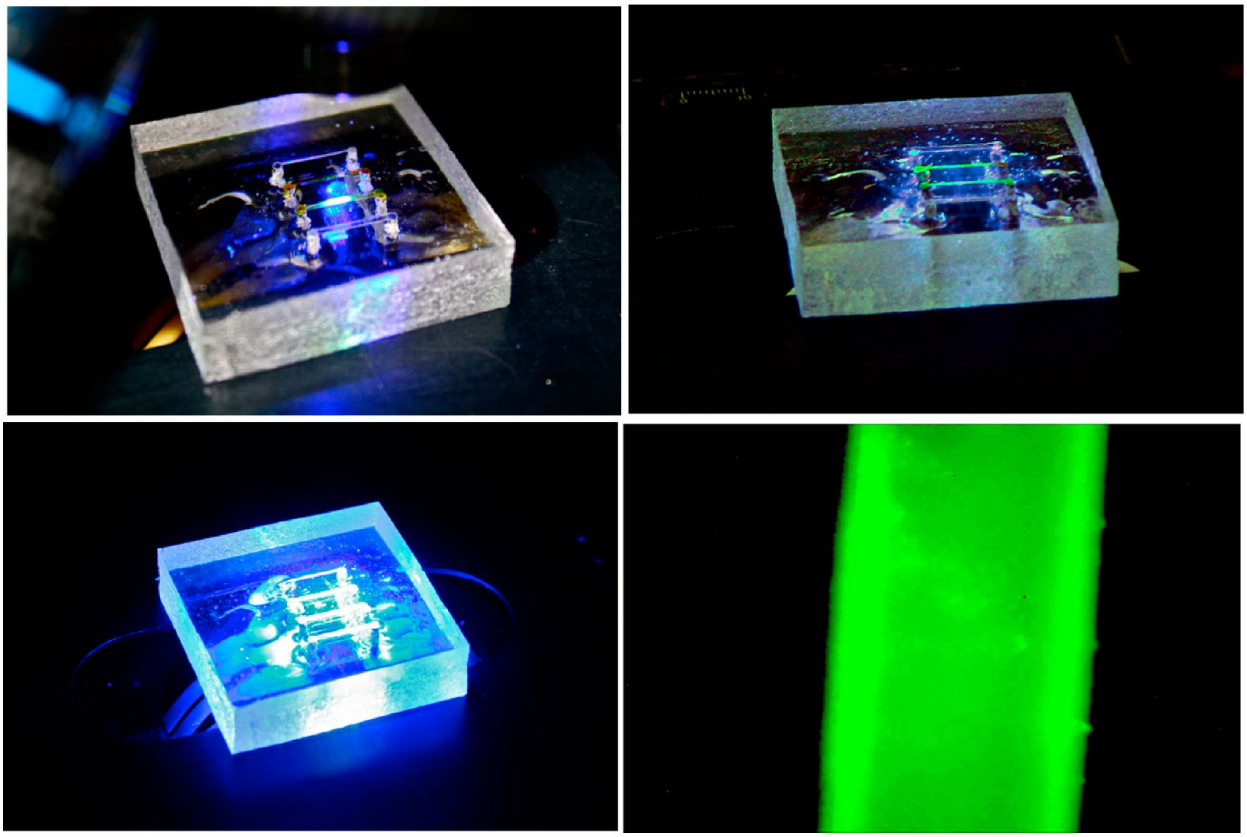

Figure 10. Fluorescent images of PETA-co-TMPTMP microfluidic devices containing an aqueous fluorescein isothiocyanate (FITC) solution. Photographic images of microchannels containing the FITC solution are shown on top and bottom left and top right, and a fluorescent microscopy image is shown on the bottom right.

resistance. This could be very beneficial in the field of microfluidics as solvent limitations normally experienced by other elastomeric materials could be eliminated.

Final, Bonded PETA-co-TMPTMP Microfluidic Devices. Multiple final microfluidic devices were prepared using the soft lithography technique coupled with the partial polymerization/excess monomer annealing technique. Some of these devices are shown in Figure 9. Prior to the bonding process, holes were drilled in specific places on the half of the device containing the microchannels via a drill press and a small drill bit. This drilling step produced holes used to attach capillaries by which the fluid would be introduced to the microfluidic device. Blunt needles bent at 90° angles, over which rubber tubing was stretched, were inserted into the holes, and a rapidly curing, two-part epoxy was used to append the needles and capillary tubing to the microfluidic device (Figure 9 top right). These capillaries were used to push aqueous fluids easily through the small hydrophilic microchannels. In some cases, polyether ether ketone (PEEK) flexible, thermoplastic tubing with an outside diameter (OD) approximately equal to the internal diameter (ID) of the predrilled holes was inserted directly, without the support of a blunt needle and requiring no epoxy to append the tubing to the device (Figure 9 bottom). An aqueous methyl orange solution was easily flowed through the microchannels. Both the epoxy-bound rubber/blunt needle capillary microfluidic device and the PEEK tubing device showed no signs of leakage. These images in Figure 9 illustrate the successful production and application of proven, stable, hydrophilic thiol–acrylate microfluidic devices capable of flowing aqueous materials down small microchannels with no leakage of the aqueous solution from the microfluidic device.

Fluorescence Microscopy Potential and Capabilities. As fluorescence microscopy is an important tool in the field of microfluidics,[80−84] it was nearly imperative that the thiol–acrylate materials have the potential to be used in such fluorescence experimentation. To prove their capabilities, an aqueous fluorescein isothiocyanate (FITC) solution was flowed through the microfluidic device and observed using simple photography and a fluorescence microscope.

Figure 10 illustrates multiple photographic images (top and bottom left and top right) of the microchannels fluorescing under the light source causing the green coloring effect. The bottom right picture in Figure 10 illustrates a fluorescent microscope image showing the microchannel fluorescing on a microscopic scale. This indicates that fluorescence microscopy could be used to analyze aqueous specimens when flowed through these thiol–acrylate microfluidic devices.

CONCLUSIONS

Novel, cost-efficient thiol–acrylate microfluidic devices with native stable hydrophilic surfaces were prepared via a soft lithography technique in less than 24 h at room temperature and ambient pressure without sophisticated instrumentation. This research was fueled by the strong need for stable hydrophilic surfaces in a field of microfluidics that is dominated by other complicated and expensive techniques that require modification to achieve only transient surface energies. The chemistry employed to produce these polymeric materials involved two consecutive Michael additions. An in situ tertiary

amine catalyst molecule was first prepared via the Michael addition of a secondary amine to a trifunctional acrylate. This molecule was then used as both a catalyst and a comonomer in an amine catalyzed thiol−acrylate Michael reaction. Because the catalyst molecule was incorporated into the polymer network, there was no need to remove it in the final steps of the reaction, making this reaction very beneficial for biological analysis. The kinetics of these reactions illustrated that the gel time of the systems could be manipulated depending on the amine concentration but only to a certain extent. The gel times for these materials ranged from 2 h to <20 min. The kinetic studies provided here also proved that these reactions proceeded to extremely high conversion, which is a normal aspect of amine-catalyzed thiol−acrylate reactions. This high conversion is another beneficial facet of the reaction in terms of biological assays as high conversion translates into fewer small-molecular weight free monomer molecules capable of escaping and disrupting biological processes.

It was found in this study that many of the properties of the material could be manipulated via a change in the amine concentration. Due to the in situ nature of the catalyst used in this system, an increase in the amine concentration resulted in a decrease in the cross-link density. The cross-link density affected many of the material properties such as strength, flexibility, and glass transition temperature. The strength and flexibility of the materials were found to be adequate, and the glass transition temperatures indicated an applicable temperature range for microfluidic assays. These novel thiol−acrylate microfluidic materials were bonded via a partial polymerization technique utilizing excess monomers on opposing sides and the same versatile thiol−acrylate chemistry and in situ tertiary amine. This added another advantage, as other techniques require expensive equipment for bonding of microfluidic devices. The strength of the bond was investigated via orthogonal delamination analysis, and it was concluded that 40% excess monomer on either surface was adequate to produce a bond strength comparable to that of PDMS surfaces bound by a traditional oxygen plasma surface activation technique.

These hydrophilic PETA-co-TMPTMP microfluidic devices exhibited native water contact angles between 60 and 65°. The native high-energy surfaces were found to be extremely stable for at least 2.5 months. This is extremely beneficial for microfluidic applications as it allows for microfluidic devices with long shelf lives. The thiol−acrylate materials were found to be highly resilient in both aqueous and organic solvents, demonstrating low solvent uptake over extended periods of time. The replication efficiency of these materials via soft lithography was found to be extremely high with capabilities of reaching structures even smaller than those utilized in this study. Final devices were prepared and observed via fluorescence microscopy. It was concluded that these devices perform very well when fluorescent dyes are flowed though the microchannels, and they are capable of being used in fluorescence microscopy studies, which are useful in the field of microfluidics.

■ ASSOCIATED CONTENT

Supporting Information

Detailed procedures used in this research; NMR data supporting the production of the in situ bound catalyst as well as FTIR data supporting the second Michael addition and the monomer conversion; further hydrophilicity, solvent uptake, and channel replication. This information is available free of charge via the Internet at http://pubs.acs.org/.

■ AUTHOR INFORMATION

Corresponding Author

*E-mail: john@pojman.com.

Notes

The authors declare no competing financial interest.

■ ACKNOWLEDGMENTS

Financial support for this work was provided by the National Science Foundation (CHE-0719099) and was greatly appreciated. Many collaborators are acknowledged for their advice and the use of their instrumentation, including Daniel Hayes, Steven Soper, Robin McCarley, Qinglin Wu, and Rafael Cueto.

■ REFERENCES

(1) Chan, J. W.; Wei, H.; Zhou, H.; Hoyle, C. E. *Eur. Polym. J.* **2009**, *45*, 2717.
(2) Hoyle, C. E.; Lee, T. Y.; Roper, T. *J. Poly. Sci., Part A: Polym. Chem.* **2004**, *52*, 5301.
(3) Hoyle, C. E.; Bowman, C. N. *Angew. Chem., Int. Ed.* **2009**, *49*, 1540.
(4) Jacobine, A. F. In *Radiation Curing in Polymer Science and Technology*; Fouassier, J. P., Ed.; Elsevier: New York, 1993; p 219.
(5) Cramer, N. B.; Scott, J. P.; Bowman, C. N. *Macromolecules* **2002**, *35*, 5361.
(6) Roper, T. M.; Kwee, T.; Lee, T.; Guymon, A. C.; Hoyle, C. E. *Polymer* **2004**, *45*, 2921.
(7) Wei, H.; Senyurt, A. F.; Jonsson, S.; Hoyle, C. E. *J. Poly. Sci., Part A: Polym. Chem.* **2007**, *45*, 822.
(8) Cramer, N. B.; Davies, T.; O'Brein, A. K.; Bowman, C. N. *Macromolecules* **2003**, *35*, 5361.
(9) Cramer, N. B.; Reddy, S. K.; Cole, M.; Hoyle, C.; Bowman, C. N. *J. Poly. Sci., Part A: Polym. Chem.* **2004**, *42*, 5817.
(10) Kade, M. J.; Burke, D. J.; Hawker, C. J. *J. Polym. Sci., Part A: Polym. Chem.* **2010**, *48*, 743.
(11) Zienty, F. B.; Schleppnik, A. A.; Vineyard, B. D. *J. Org. Chem.* **1962**, *27*, 3140.
(12) Rim, C.; Lahey, L. J.; Patel, V. G.; Zhang, H. M.; Son, D. Y. *Tetrahedron Lett.* **2009**, *50*, 745.
(13) Mather, B. D.; Viswanathan, K.; Miller, K. M.; Long, T. E. *Prog. Polym. Sci.* **2006**, *31*, 487.
(14) Rizzi, S. C.; Hubbell, J. A. *Biomacromolecules* **2005**, *6*, 1226.
(15) Chan, J. W.; Hoyle, C. E.; Lowe, A. B.; Bowman, M. *Macromolecules* **2010**, *43*, 6381.
(16) Hu, G.; Pojman, J. A.; Bounds, C.; Taylor, A. F. *J. Polym. Sci., Part A: Polym. Chem.* **2010**, *48*, 2955.
(17) Khire, V. S.; Lee, T. Y.; Bowman, C. N. *Macromolecules* **2007**, *40*, 5669.
(18) Lee, T.; Kaung, W.; Jönsson, S.; Lowery, K.; Guymon, C.; Hoyle, C. *J. Poly. Sci., Part A: Polym. Chem.* **2004**, *42*, 4424.
(19) Khire, V. S.; Kloxin, A. M.; Couch, C. L.; Anseth, K. S.; Bowman, C. N. *J. Polym. Sci., Part A: Polym. Chem.* **2008**, *46*, 6896.
(20) Clark, T.; Kwisnek, L.; Hoyle, C. E.; Nazarenko, S. *J. Polym. Sci., Part A: Polym. Chem.* **2009**, *47*, 14.
(21) Sanui, K.; Ogata, N. *Bull. Chem. Soc. Jpn.* **1967**, *40*, 1727.
(22) Shin, J.; Matsushima, H.; Chan, J. W.; Hoyle, C. E. *Macromolecules* **2009**, *42*, 3294.
(23) Chan, J. W.; Yu, B.; Hoyle, C. E.; Lowe, A. B. *Chem. Commun.* **2008**, 4959.
(24) Bounds, C. O.; Goetter, R.; Pojman, J. A.; Vandersall, M. *J. Polym. Sci., Part A: Polym. Chem.* **2012**, *50*, 409.
(25) Whitesides, G. M. *Nature* **2006**, *442*, 368.
(26) Lin, C. C.; Wang, J. H.; Wu, H. W.; Lee, G. B. *Jala* **2010**, *15*, 253.
(27) Sia, S. K.; Whitesides, G. M. *Electrophoresis* **2003**, *24*, 3563.

(28) Lenigk, R.; Liu, R. H.; Athavale, M.; Chen, Z. J.; Ganser, D.; Yang, J. N.; Rauch, C.; Liu, Y. J.; Chan, B.; Yu, H. N.; Ray, M.; Marrero, R.; Grodzinski, P. *Anal. Biochem.* **2002**, *311*, 40.
(29) Dimalanta, E. T.; Lim, A.; Runnheim, R.; Lamers, C.; Churas, C.; Forrest, D. K.; de Pablo, J. J.; Graham, M. D.; Coppersmith, S. N.; Goldstein, S.; Schwartz, D. C. *Anal. Chem.* **2004**, *76*, 5293.
(30) Chiem, N. H.; Harrison, D. J. *Electrophoresis* **1998**, *19*, 3040.
(31) Badal, M. Y.; Wong, M.; Chiem, N.; Salimi-Moosavi, H.; Harrison, D. J. *J. Chromatogr., A* **2002**, *947*, 277.
(32) Chang, W.; Komazu, T.; Korenaga, T. *Anal. Lett.* **2008**, *41*, 1468.
(33) Reyes, D. R.; Iossifidis, D.; Auroux, P. A.; Manz, A. *Anal. Chem.* **2002**, *74*, 2623.
(34) Auroux, P. A.; Iossifidis, D.; Reyes, D. R.; Manz, A. *Anal. Chem.* **2002**, *74*, 2637.
(35) Manz, A.; Harrison, D. J.; Verpoorte, E. M. J.; Fettinger, J. C.; Paulus, A.; Ludi, H.; Widmer, H. M. *J. Chromatogr.* **1992**, *593*, 253.
(36) Yoon, T. H.; Lee, H. J.; Yan, J.; Kim, D. P. *J. Ceram. Soc. Jpn.* **2006**, *114*, 473.
(37) Waldbaur, A.; Rapp, H.; Lange, K.; Rapp, B. E. *Anal. Methods* **2011**, *3*, 2681.
(38) Becker, H.; Gartner, C. *Electrophoresis* **2000**, *21*, 12.
(39) Becker, H.; Gartner, C. *Anal. Bioanal. Chem.* **2008**, *390*, 89.
(40) Lee, S.; Kang, H. S.; Park, J. K. *Adv. Mater.* **2012**, *24*, 2069.
(41) Zorlutuna, P.; Annabi, N.; Camci-Unal, G.; Nikkhah, M.; Cha, J. M.; Nichol, J. W.; Manbachi, A.; Bae, H. J.; Chen, S. C.; Khademhosseini, A. *Adv. Mater.* **2012**, *24*, 1782.
(42) Valiokas, R. *Cell. Mol. Life Sci.* **2012**, *69*, 347.
(43) Xue, L. J.; Zhang, J. L.; Han, Y. C. *Prog. Polym. Sci.* **2012**, *37*, 564.
(44) Huh, D.; Hamilton, G. A.; Ingber, D. E. *Trends Cell Biol.* **2011**, *21*, 745.
(45) Pan, J.; Chan, S. Y.; Lee, W. G.; Kang, L. F. *Biotechnol. J.* **2011**, *6*, 1477.
(46) Hahm, J. I. *J. Biomed. Nanotechnol.* **2011**, *7*, 731.
(47) Ng, J. M. K.; Gitlin, I.; Stroock, A. D.; Whitesides, G. M. *Electrophoresis* **2002**, *23*, 3461.
(48) Grover, W. H.; Skelley, A. M.; Liu, C. N.; Lagally, E. T.; Mathies, R. A. *Sens. Actuators, B: Chem.* **2003**, *89*, 315.
(49) Eddings, M. A.; Gale, B. K. *J. Micromech. Microeng.* **2006**, *16*, 2396.
(50) Johnson, M.; Liddiard, G.; Eddings, M.; Gale, B. *J. Micromech. Microeng.* **2009**, 19.
(51) Zhou, J. W.; Ellis, A. V.; Voelcker, N. H. *Electrophoresis* **2010**, *31*, 2.
(52) van Poll, M. L.; Zhou, F.; Ramstedt, M.; Hu, L.; Huck, W. T. S. *Angew. Chem., Int. Ed.* **2007**, *46*, 6634.
(53) Mata, A.; Fleischman, A. J.; Roy, S. *Biomed. Microdevices* **2005**, *7*, 281.
(54) de Menezes Atayde, C.; Doi, I. *Phys. Status Solidi C* **2010**, *7*, 189.
(55) Patrito, N.; McCague, C.; Norton, P. R.; Petersen, N. O. *Langmuir* **2007**, *23*, 715.
(56) Hu, S. W.; Ren, X. Q.; Bachman, M.; Sims, C. E.; Li, G. P.; Allbritton, N. L. *Langmuir* **2004**, *20*, 5569.
(57) Lahann, J.; Balcells, M.; Lu, H.; Rodon, T.; Jensen, K. F.; Langer, R. *Anal. Chem.* **2003**, *75*, 2117.
(58) Phillips, K. S.; Cheng, Q. *Anal. Chem.* **2005**, *77*, 327.
(59) Rolland, J. P.; Van Dam, R. M.; Schorzman, D. A.; Quake, S. R.; DeSimone, J. M. *J. Am. Chem. Soc.* **2004**, *126*, 2322.
(60) Séguin, C.; McLachlan, J. M.; Norton, P. R.; Lagugné-Labarthet, F. *Appl. Surf. Sci.* **2010**, *256*, 2524.
(61) Bodas, D.; Khan-Malek, C. *Microelectron. Eng.* **2006**, *83*, 1277.
(62) Bodas, D.; Rauch, J. Y.; Khan-Malek, C. *J. Appl. Polym. Sci.* **2011**, *120*, 1426.
(63) Bodas, D. S.; Khan-Malek, C. *Sens. Actuators, B: Chem.* **2007**, *120*, 719.
(64) Gao, C. Y.; Guo, Y. Y.; He, J.; Wu, M.; Liu, Y.; Chen, Z. L.; Cai, W. S.; Yang, Y. L.; Wang, C.; Feng, X. Z. *J. Mater. Chem.* **2012**, *22*, 10763.
(65) Lee, D.; Yang, S. *Sens. Actuators, B: Chem.* **2012**, *162*, 425.
(66) Li, J. Y.; Wang, M.; Shen, Y. B. *Surf. Coat. Technol.* **2012**, *206*, 2161.
(67) Wu, Z. Q.; Tong, W. F.; Jiang, W. W.; Liu, X. L.; Wang, Y. W.; Chen, H. *Colloids Surf., B: Biointerfaces* **2012**, *96*, 37.
(68) Yao, M. J.; Fang, J. *J. Micromech. Microeng.* **2012**, *22*, 025012.
(69) Chiou, B. S.; Khan, S. A. *Macromolecules* **1997**, *30*, 7322.
(70) Brigo, L.; Carofiglio, T.; Fregonese, C.; Meneguzzi, F.; Mistura, G.; Natali, M.; Tonellato, U. *Sens. Actuators, B: Chem.* **2008**, *130*, 477.
(71) Cygan, Z. T.; Cabral, J. T.; Beers, K. L.; Amis, E. J. *Langmuir* **2005**, *21*, 3629.
(72) Natali, M.; Begolo, S.; Carofiglio, T.; Mistura, G. *Lab Chip* **2008**, *8*, 492.
(73) Cabral, J. T.; Hudson, S. D.; Harrison, C.; Douglas, J. F. *Langmuir* **2004**, *20*, 10020.
(74) Good, B. T.; Bowman, C. N.; Davis, R. H. *Lab Chip* **2006**, *6*, 659.
(75) Ashley, J. F.; Cramer, N. B.; Davis, R. H.; Bowman, C. N. *Lab Chip* **2011**, *11*, 2772.
(76) Besson, E.; Gue, A. M.; Sudor, J.; Korri-Youssoufi, H.; Jaffrezic, N.; Tardy, J. *Langmuir* **2006**, *22*, 8346.
(77) Dickey, M. D.; Collister, E.; Raines, A.; Tsiartas, P.; Holcombe, T.; Sreenivasan, S. V.; Bonnecaze, R. T.; Willson, C. G. *Chem. Mater.* **2006**, *18*, 2043.
(78) Crowe, J. A.; Genzer, J. *J. Am. Chem. Soc.* **2005**, *127*, 17610.
(79) Odian, G. *Principles of Polymerization*, 4th ed.; Wiley: New York, 2004.
(80) Luo, Y.; Liu, C.; Qu, Y. Y.; Fang, N. *Bioanalysis* **2012**, *4*, 453.
(81) Jiang, L. G.; Zeng, Y.; Zhou, H. B.; Qu, J. A. Y.; Yao, S. H. *Biomicrofluidics* **2012**, *6*, 012810.
(82) Foley, C. P.; Nishimura, N.; Neeves, K. B.; Schaffer, C. B.; Olbricht, W. L. *Ann. Biomed. Eng.* **2012**, *40*, 292.
(83) Burgess, J. G. *Curr. Opin. Biotechnol.* **2012**, *23*, 29.
(84) Batabyal, S.; Rakshit, S.; Kar, S.; Pal, S. K. *Rev. Sci. Instrum.* **2012**, *83*, 043113.